Short-Term Photovoltaic Power Forecasting Using a Neural Network Dynamic Time Series

Thatree Mamee
King Mongkut’s University of Technology Thonburi (KMUTT) Bangkok

Usa Boonbumrung
King Mongkut’s University of Technology Thonburi (KMUTT) Bangkok

Netithorn Ditnin
King Mongkut’s University of Technology Thonburi (KMUTT) Bangkok

Patamaporn Sripadungtham
Department of Electrical Engineering Kasetsart University Bangkok

他

https://doi.org/10.5109/7323261

出版情報：Proceedings of International Exchange and Innovation Conference on Engineering & Sciences (IEICES). 10, pp.183-189, 2024-10-17. International Exchange and Innovation Conference on Engineering & Sciences
バージョン：

Short-Term Photovoltaic power forecasting Using a Neural Network dynamic time series.

Thatree Mamee[1], Usa Boonbumrung[1], Netithorn Ditnin[1], Patamaporn Sripadungtham [2], Nitikorn Nanthawirojsiri[1]
[1] King Mongkut's University of Technology Thonburi (KMUTT) Bangkok, Thailand,
[2] Department of Electrical Engineering Kasetsart University Bangkok, Thailand

Corresponding author email: thatree.mam@kmutt.ac.th

Abstract: *Currently, short-term photovoltaic (PV) power forecasting is crucial for optimizing PV power operation in both off-grid and grid-connected systems. This paper compares different PV power forecasting models: Nonlinear Autoregressive (NAR), Nonlinear Input-Output (NIO), and Nonlinear Autoregressive with External Input (NARX) for a PV rooftop 23.1 kWp. The primary input data consists of solar irradiance and temperatures from 1 to 6 hours before the present time. The training process utilizes one year of data (2019) to develop the learning model. Data from January 2020 to April 2020 were used to test the models. This paper reports the optimized time series and number of neurons, with MAPE and R^2 used as accuracy indicators for evaluating the models. The best model, NARX achieved MAPE=6.84% and R^2=0.9 with a time series delay of 3 hours and 50 neurons.*

Keywords: Irradiance forecasting, Neural network, Solar cell systems

1. INTRODUCTION

In Thailand, solar rooftop installations have seen significant growth over the past decade across various building types, including commercial, industrial, governmental, public institutions (such as schools and hospitals), and residential buildings. By 2019, the country had installed 45,540 ktoe (11,630 MWh) of solar rooftop capacity. To support Thailand's energy policy, the Metropolitan Electricity Authority (MEA) has incentivized the installation of solar rooftop systems for self-consumption in residential buildings. In 2020, the Thai government introduced a policy allowing excess power generated by solar rooftops (beyond self-consumption) to be sold back to the grid at a compensation rate of 1.68 THB per unit. However, this rate is lower than the electricity cost of 5.2674 THB per unit during peak periods and 2.1827 THB per unit during off-peak periods for the Time of Use (TOU) rate [1],[2]. Consequently, bill savings for households with installed PV systems depend on the relationship between solar irradiance, load profile, and electricity tariffs. Effective energy management is thus crucial for reducing electrical energy costs.

Renewable energy can be harnessed from natural sources such as solar radiation, wind, and biomass [3]. This research focuses on the output power of photovoltaic (PV) systems, which is influenced by environmental factors like solar irradiance, temperature, and weather conditions. To optimize the utility of PV systems, it is essential to plan and evaluate projects through design and optimized control techniques [4-5]. Additionally, considerations of load profile and energy storage management are critical. Various models have been employed to forecast PV power [6-7], aiming to enhance the performance of solar systems by improving operation scheduling and capacity optimization. PV power forecasting can be categorized into three types: long-term (one month to one year), medium-term (one week to one month), and short-term (one week or less).

In previous work, forecasting models need several input variables to achieve high accuracy. These inputs are wind speed, Temperature, Humidity, Global horizontal radiation, diffuse horizontal radiation, Wind direction, and Current phase average based on deep learning neural network [6]. Another one is PV output power(P), global horizontal radiation (GHR), diffuse horizontal radiation (DHR), ambient temperature (AT), wind speed (WS), and relative humidity (RH) with the hybrid deep learning model [7]. It means the user needs many sensors and a high level of sensors to collect the data. Therefore, it is not proper for the local user to use in small systems such as house solar rooftops due to the high cost of system investment.

This paper proposes PV power forecasting using the input parameters are Solar Irradiance and Ambient temperature from only 2 sensors. To investigate the accuracy of short-term PV power forecasting with a few input parameters. The primary objective is to assess the accuracy of short-term PV power forecasting with minimal input parameters and its applicability in real cases. The study focuses on a one-hour-ahead forecasting model, classified as short-term forecasting. The research utilizes three Neural Network dynamic time series models to identify the best-performing model. The study compares the different input sizes and calculates training times to assess accuracy and training duration for practical applications. The relationship between power forecasting accuracy and the number of input variables is considered in training time series models.

Furthermore, the research evaluates and tests the optimal number of neurons and input delay times to determine the most effective configurations, including three types of time series models that can be applied with varying amounts of input data.

The result shows that the model used 2 parameters from 2 sensors (Irradiance and ambient temperature) has high accuracy in predicting sunny days. However, on a cloudy day, the error increases to 18%, and on a rainy day is a high error at about 50%.

2. NEURAL NETWORKS BACKGROUND

Neural networks can be divided into two categories: static and dynamic networks. The output from a static neural network (SNN) is calculated directly from the input through feedforward networks, without feedback elements or delays. In contrast, the output from a dynamic neural network (DNN) depends not only on the present input but also on delayed inputs or states of the network [8]. DNNs can be further divided into feedforward-dynamic neural networks (FDNN) and recurrent-dynamic neural networks (RDNN).

2.1 Feedforward-dynamic neural networks (FDNN)

In the structure of an FDNN, as shown in Fig. 1, the input networks contain delays in the sequence of input vectors with a certain time order. The network input is processed by the present time u(t) and delay time u(t−n). The output is the future value y(t+1). The model can incorporate multiple hidden layers to form a multi-layer perceptron, thus increasing the dimensionality of the network [9-11]. The feedforward-dynamic networks can be calculated by the following equation (1).

$$y(t+1) = F(u(t)\cdot w_{1,1} + u(t-1)\cdot w_{1,2} + \cdots + u(t-n)\cdot w_{1,n} \quad (1)$$

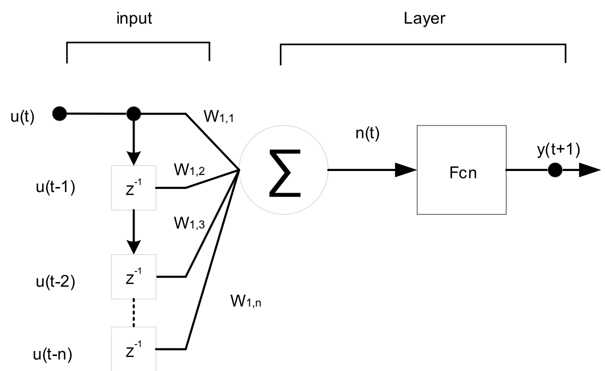

Fig.1. Simple Feedforward-dynamic networks

2.2 Recurrent-dynamic neural networks (RDNN)

RDNN structure as shown in Fig. 2, the input value given by present value u(t) that includes delays time value u(t-n) into the network sequence as same as FDNN but the output is fed back to the input via another tapped-delay-line memory. The output delay values are y(t), y(t-1), …, y(t-n) which feedback the input again to obtain the output y(t+1). The RDNN is referred to as a nonlinear autoregressive with exogenous inputs (NARX) [12] model that can be calculated by the following equation (2).

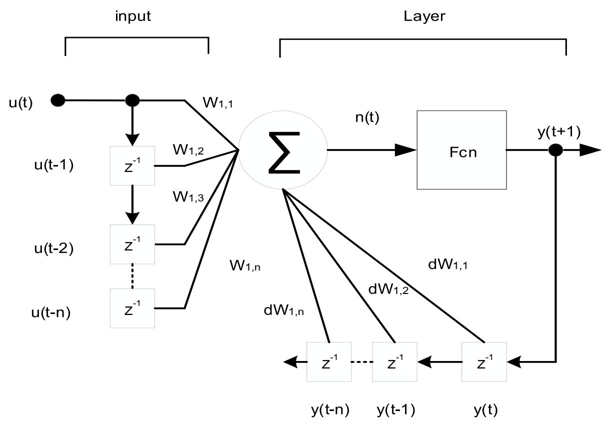

Fig. 2. Simple Recurrent-dynamic neural networks

$$y(t+1) = F(u(t)\cdot w_{1,1} + u(t-1)\cdot w_{1,2} + \cdots + u(t-n)\cdot w_{1,n} + y(t)\cdot dw_{1,1} + y(t-1)\cdot dw_{1,2} + \cdots y(t-n)\cdot dw_{1,n} \quad (2)$$

2.3 Performance indexes

To evaluate the performance of forecasting model in this paper, two accuracy estimating metrics were used in the training and testing forecasting data. There are %MAPE (Mean Absolute Percentage Error), and R2 (R Squared linear regression) as follows:

$$MBE = \%MAPE = \frac{1}{N}\left(\sum_{i=1}^{N} \left|\frac{y(i)-y'(i)}{y(i)}\right|\right) \times 100 \quad (3)$$

$$R^2 = 1 - \frac{\sum_i (y(i)-y'(i))^2}{\sum_i (y(i)-\bar{y})^2} \quad (4)$$

Where y is the actual values.
y' is the predicted value of y
and $\bar{y}$ is the mean of the y values.

3. PV POWER HOUR-AHEAD FORECASTING

3.1 Experimental Data

The historical data was collected from PV grid-connected systems in Bangkok, Thailand. The specifications of this system are shown in Table 1. Data collection included PV power output, irradiance, and ambient temperature, which were averaged and stored in the database every hour.

The dataset from the year 2019 was selected for the training model, while the dataset from January to April 2020 was selected for testing the model.

Table 1. Technical Specification of PV Grid-Connected Systems

Technical Specification	Value
Array Rating (kW)	23.1 kWp
Panel Rated Power at STC(P_{mpp})	300 W
Number of panels	77
Inverter spec	Sunny Tri-Power SMA 25000TL, 2.5kW 3phase
Panel model	Schutten STP6-300/72
Type of Tracker	Fixed
Array Tilt/Azimuth	Tilt = 13°, Azimuth = 0°

3.2 Training and testing method

In this case study, the Neural Network (NN) models were used to learn from historical data (2019) and to compare errors between input and target in order to adjust the weight in each neuron for forecasting PV power one hour ahead. After that, data from January to April 2020 were used to test the model's accuracy. The NN models were trained using the Levenberg-Marquardt back-propagation algorithm and divided into three distinct models [13-15].

The first model is the Nonlinear Auto-Regressive (NAR) model, which forecasts the series data output y(t+1) based on the present value and delay time values y(t), y(t-1), …, y(t-n)). Only irradiance data is used as input for this model.

The second model is the Nonlinear Input-Output (NIO) model, which forecasts the series output y(t+1) based on the present value and delay values u(t), u(t-1), …., u(t-n). The input data for this model includes time, temperature, and irradiance from past times.

The third model is the Nonlinear Autoregressive with External (Exogenous) Input (NARX) model, which forecasts the series output y(t+1) based on the present and delay values u(t), u(t-1), …., u(t-n). The input values and output are similar to the NIO model; however, the NARX model includes recurrent networks, where the output y(t−n) is fed back into the input network.

The experimental method is shown in Fig. 3, and the partial input data for training is shown in Fig. 4. The data separation for training and testing in this experiment is shown in Fig. 5.

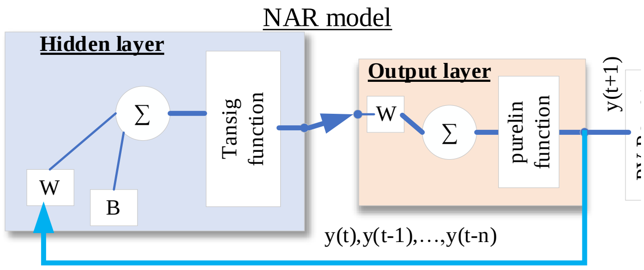

a) NAR Model

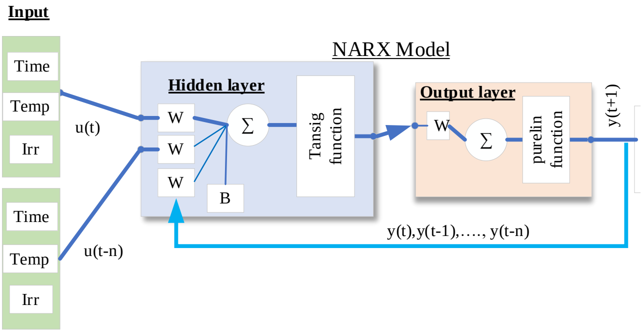

b) NARX Model

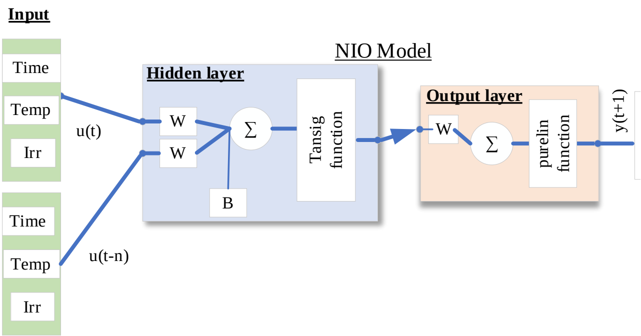

c) NIO Model

Fig. 3. The NN time series models

4. SIMULATION RESULTS AND DISCUSSIONS

To study dynamic neural networks with different models and evaluate the relationship between input and target variables, the experimental methodology was divided into three models. Each model varied the input data by adjusting the number of time delays and neurons, as detailed in Table 2.

The forecasting results were categorized into two parts: the performance of the training model and the performance of the testing model. In the training model component, the number of time delays (1-6 hours) and the number of neurons were varied to determine the optimal performance, which was evaluated using MAPE and R^2.

In the NAR model, the input dataset consisted only of solar irradiance, which varied over the time series through the Neural Network model. The number of neurons in the hidden layer was adjusted to calculate the best learning performance. In the NARX and NIO models, the input data included additional variables such as days, months, hours, temperature, and solar irradiance.

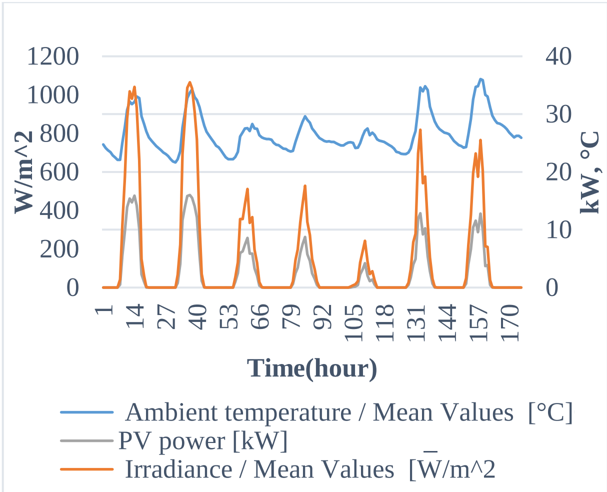

Fig. 4. partial input and target data for training

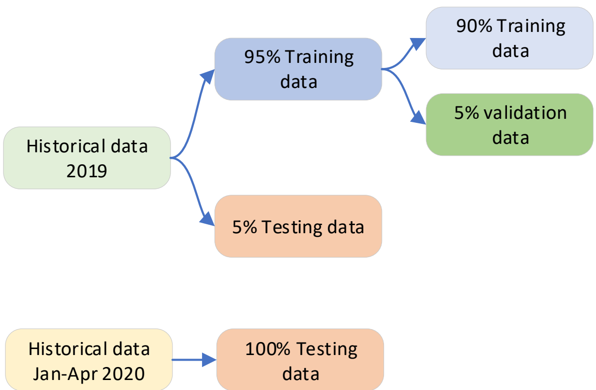

Fig. 5. The data division criterion for training model

4.1 Training result

The training performance was evaluated based on learning accuracy using various input data and different models. The results indicate that the NARX and NIO models outperform the NAR model in the learning process, as shown in Fig. 6. Specifically, the NARX model performs the forecasting error (MAPE) less than the NIO model due to its recurrent output function for iterative training.

To analyze the influence of input data with various delay times, it is important to consider both accuracy and training time. This comparison helps weigh the advantages and disadvantages and determine the reasons for selecting the proper models and input data.

As the NAR model, at the time deley1 is presented the lower accuracy than NARX. However, the NAR training time process has a good result compared with NARX in condition large data input and large number of neurons as shown in Fig.7.

Although NARX has forecasting error (MAPE) less than NIO model, however, if considering the training time process, NIO is faster than NARX. In the same way, increasing the number of neurons achieves the enhancement of accuracy as shown in Fig.6. On the other hand, it will increase the training time process as shown in Fig.7.

Table 2. Experimental methodology process for learning model

Model	input	time delay (Hour)	Vary number of neurons	output
NAR	Irradiance	1-6	50,100,200 ,500	PV power
NARX	Day Month Hour Temperature Irradiance	1-6	50,100,200 ,500	PV power
NIO	Day Month Hour Temperature Irradiance	1-6	50,100,200 ,500	PV power

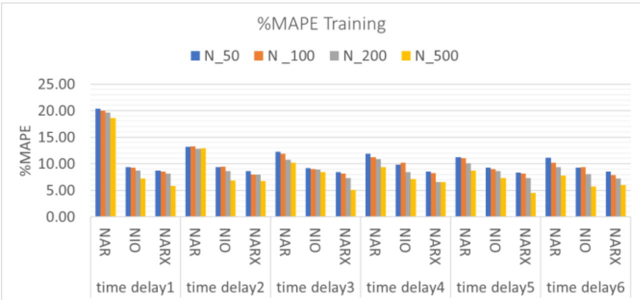

(a) MAPE

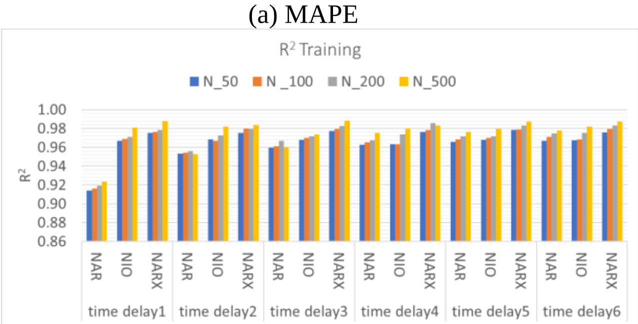

(b) R^2

Fig.6 Training performance evaluations of different model methods

4.2 Testing Result

The testing model utilized weight values and activation functions obtained from the training model trained on the dataset from the year 2019. The input dataset (January to April 2020) was used for testing to ensure that the testing data had never been seen or memorized by the model before, as depicted in Fig. 5.

The best accuracy from each model is presented below:

-NAR testing using a time series delay of 4 hours, number of neurons 50, MAPE 9.03, R^2=0.97 as shown in Fig. 9a, the most error is at -0.34 kW shown in Fig. 10a.

-NIO testing NIO model use time series delay 3 hours, number of neurons 50, MAPE=7.3477, R^2=0.98 as shown in Fig. 9b, the most error is at -0.34 kW as shown in Fig. 10b.

-NARX testing use time series delay 3 hours, number of neurons 50, MAPE=6.84, R^2=0.98 as shown in Fig. 9c, the most error is at -0.34 kW as shown in Fig. 10c.

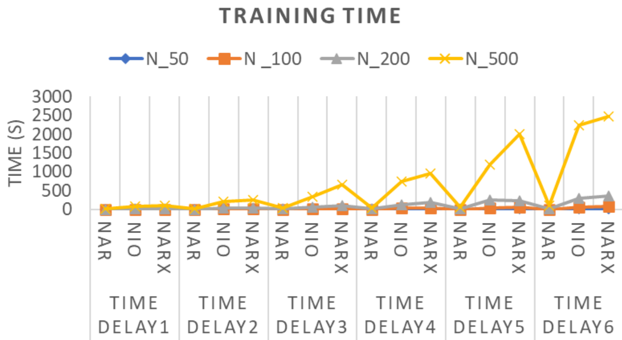

Fig. 7. Training process time in a different model (N_x is the number of neurons)

As a result, it was found that the NAR model used a small input dataset but achieved very low accuracy. Its accuracy can be improved by increasing the number of time delays. In contrast, the NARX and NIO models demonstrate high performance even with a single time delay input. Furthermore, accuracy improves with an increasing number of time delays, as shown in the results in Fig. 7 and Fig. 8.

Considering the number of neurons, the results indicate that increasing the number of neurons enhances training accuracy. However, in testing, the opposite trend is observed: the model with 500 neurons shows lower accuracy compared to models with other numbers of neurons due to overfitting during training.

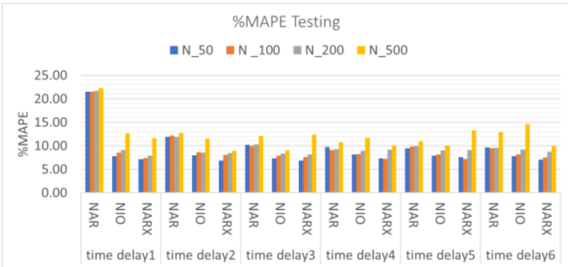

(a) MAPE

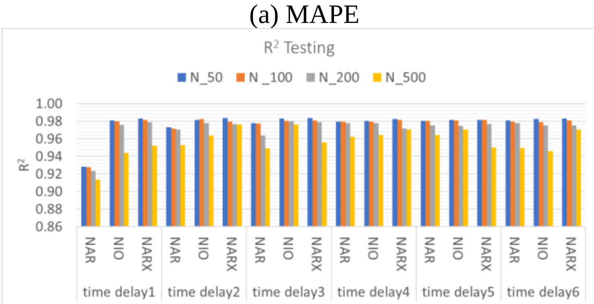

(b) R^2

Fig. 8. Testing performance evaluations of different model methods

To evaluate the sensitivity influenced by weather conditions, two cases were considered: Sunny days and Cloudy/Rainy days, as shown in Fig. 11 and Fig. 12 respectively. The results indicate that the models achieve high accuracy in predicting PV power on sunny days, with less than 4% errors in both the NARX and NIO models. However, on cloudy days, the error increases to 18%, and on rainy days, the error significantly worsens to approximately 50%, as shown in Table 3.

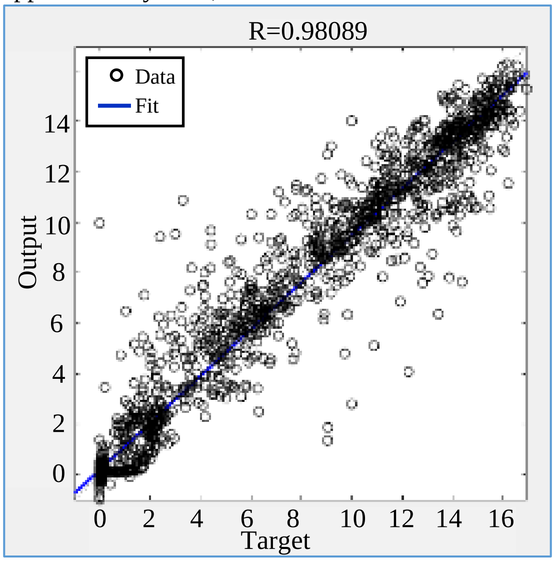

a)

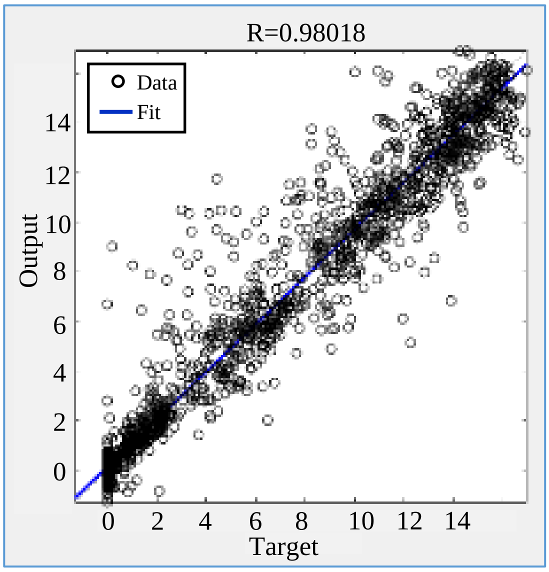

b)

R=0.98227

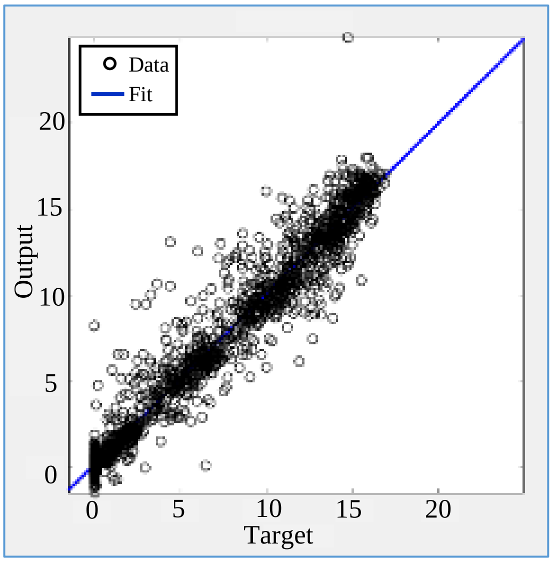

c)

Fig. 9. Linear regression Testing result a) NAR b) NIO c) NARX

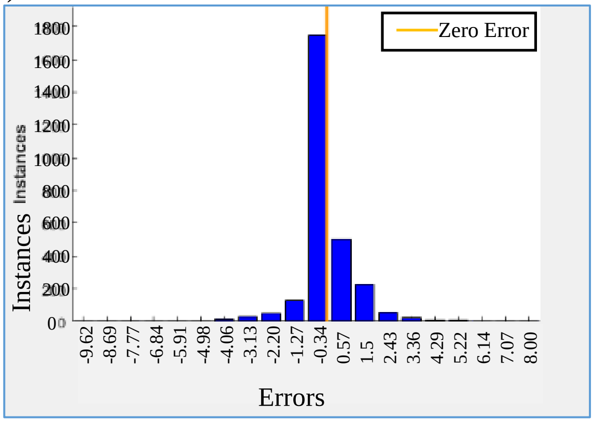

a)

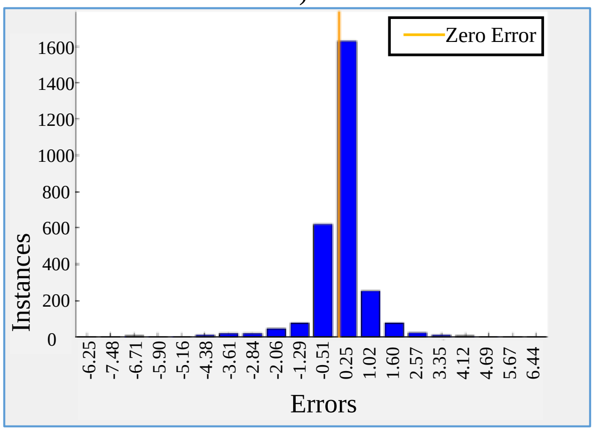

b)

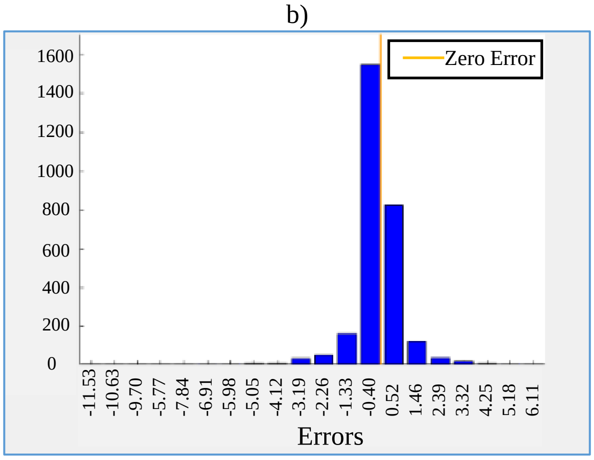

c)

Fig. 10. Error Histogram Testing Result a) NAR b) NIO c) NARX

Table 3 MAPE for testing data in a sunny day

	MAPE_NAR (%)	MAPE_NARX (%)	MAPE_NIO (%)
Day1sunny day	6.00	2.56	3.70
Day2sunny day	5.03	3.47	3.58
Day3sunny day	5.29	3.76	2.95
Day1 Rainy	51.96	44.88	49.07
Day2Cloudy/ Rainy	24.04	18.63	15.98
Day3Cloudy/ Rainy	17.98	13.87	12.89

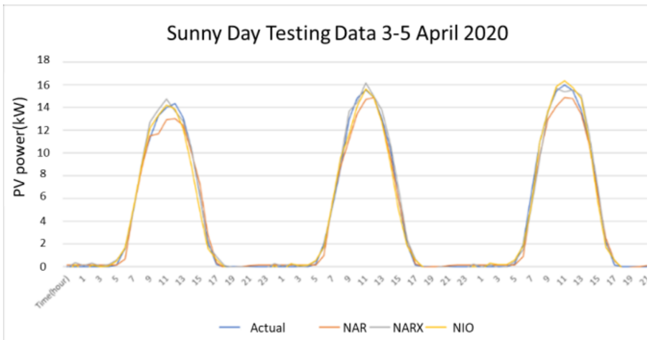

Fig. 11 PV power forecasting result for testing data in a Sunny Day

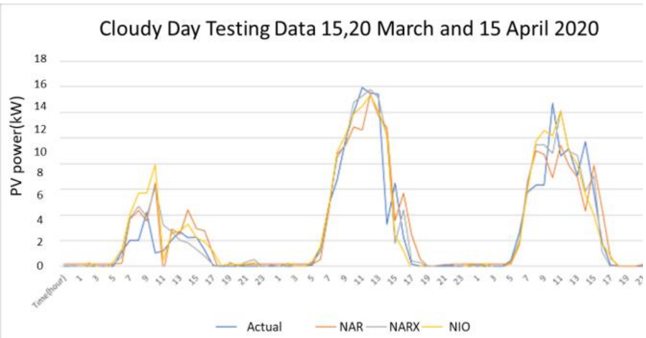

Fig. 12. PV power forecasting result for testing data in a Cloudy/Rainy Day

5. Conclusion

This study proposes PV power forecasting using simple input parameters irradiance and temperature. Three models NAR, NIO, and NARX were utilized to determine the most effective model for forecasting PV power. The forecasting results were evaluated under varying input time series lengths and numbers of neurons. According to the experimental findings, the NARX model exhibited the highest performance due to its superior ability to learn and memorize historical datasets compared to the NAR and NIO models. The best performing NARX model used five input variables (Day, Month, Hour, Temperature, and Irradiance) with a time sequence delay of three hours and 50 neurons. Factors influencing forecasting accuracy included the size of the training dataset, data precision, and the model's capability to recognize patterns. While the forecasting model demonstrated high accuracy on sunny days and moderate accuracy on cloudy days, its accuracy diminished during rainy days.

6. ACKNOWLEDGMENT

This paper would not have been possible without the data support by Dr. Terapol Pruksathorn's house which photovoltaic on grid and storage systems. We wish to express our profound gratitude to Dr. Terapol Park Sathorn for their indispensable contributions, which have significantly bolstered the success of this research endeavor. Your unwavering support has been instrumental in our pursuit of academic excellence. Thank you sincerely for your invaluable assistance.

This project is funded by National Research Council of Thailand (NRCT) and Electricity Generating Authority of Thailand (EGAT)

7. REFERENCES

[1] A. Chaianong, S. Tongsopit, A. Bangviwat, and C. Menke, "Bill saving analysis of rooftop PV customers and policy implications for Thailand," Renew. Energy, vol. 131, pp. 422–434, Feb. 2019, doi: 10.1016/j.renene.2018.07.057.

[2] Metropolitan electricigy authority, "Electricity rate," https://www.mea.or.th/, 2020. https://www.mea.or.th/profile/161/164.K. Elissa, "Title of paper if known," unpublished.

[3] H. Farzaneh, Ushering in a new age of urban energy efficiency and low emission societies, IEICES. (2021)

[4] N. Ul Rehman, F. Hooman, "Techno-Economic Analysis of on Grid PV Power System for Vocational Training Institute in Baluchistan Pakistan to Reduce the Cost of Energy", IEICES. (2022)

[5] A. Das Avi, et al. "Optimization of Solar, Wind and Biomass-Based Hybrid Renewable Energy System in St. Martin ' s Island, Bangladesh" , IEICES. (2021).

[6] K. Wang, X. Qi, and H. Liu, "A comparison of day-ahead photovoltaic power forecasting models based on deep learning neural network," Appl. Energy, vol. 251,Oct.2019,doi:10.1016/j.apenergy.2019.113315. Y. Yorozu, M. Hirano, K. Oka, and Y. Tagawa, "Electron spectroscopy studies on magneto-optical media and plastic substrate interface," IEEE Transl. J. Magn. Japan, vol. 2, pp. 740–741, August 1987 [Digests 9th Annual Conf. Magnetics Japan, p. 301, 1982].

[7] P. Li, K. Zhou, X. Lu, and S. Yang, "A hybrid deep learning model for short-term PV power forecasting," Appl. Energy, vol. 259, Feb. 2020, doi: 10.1016/j.apenergy.2019.114216

[8] M. Hudson, B. Martin, T. Hagan, and H. B. Demuth, "Deep Learning ToolboxTM User's Guide," 1992. [Online]. Available: www.mathworks.com.

[9] Y. M. Chiang, L. C. Chang, and F. J. Chang, "Comparison of static-feedforward and dynamic-feedback neural networks for rainfall-runoff modeling," J. Hydrol., vol. 290, no. 3–4, pp. 297–311, May 2004, doi: 10.1016/j.jhydrol.2003.12.033.

[10] J. Xu, M. C. E. Yagoub, R. Ding, and Q. J. Zhang, "Feedforward Dynamic Neural Network Technique for Modeling and Design of Nonlinear Telecommunication Circuits and Systems," 2003. doi: 10.1109/ijcnn.2003.1223815.

[11] Jung, E., & Lee, C. (2000). Dimension expansion of neural networks. 678-680. Paper presented at 2000 International Geoscience and Remote Sensing Symposium (IGARSS 2000), Honolulu, HI, USA.

[12] S. S. Haykin and S. S. Haykin, Neural networks and learning machines. Prentice Hall/Pearson, 2009.

[13] C. Lv et al., "Levenberg-marquardt backpropagation training of multilayer neural networks for state estimation of a safety-critical cyber-physical system," IEEE Trans. Ind. Informatics, vol. 14, no.

8, pp. 3436–3446, Aug. 2018, doi: 10.1109/TII.2017.2777460.

[14] S. Sapna, "Backpropagation Learning Algorithm Based on Levenberg Marquardt Algorithm," Oct. 2012, pp. 393–398, doi: 10.5121/csit.2012.2438.

[15] M. Pierro et al., "Deterministic and Stochastic Approaches for Day-Ahead Solar Power Forecasting," J. Sol. Energy Eng. Trans. ASME, vol. 139, no. 2, Apr. 2017, doi: 10.1115/1.4034823.